

## NON-LINEAR FINITE ELEMENT ANALYSIS OF SHEAR CRITICAL HIGH STRENGTH CONCRETE BEAMS

Juan SAGASETA<sup>a</sup>, Robert L. VOLLUM<sup>b</sup>

<sup>a</sup>Dr.; École Polytechnique Fédérale de Lausanne (EPFL)

<sup>b</sup>Dr.; Department of Civil & Environmental Engineering, Imperial College London Rd, Skempton Bldg. SW7 2BU, London  
E-mail address: [r.vollum@imperial.ac.uk](mailto:r.vollum@imperial.ac.uk)

Received: 01.09.09; Revised: 10.10.09; Accepted: 20.10.09

### Abstract

Experimental evidence shows that the bond between the aggregate and cement paste can be sufficiently strong in high-strength concretes for cracks to pass through the aggregate. Cracks that pass through coarse aggregate are smooth and significantly reduce the potential for shear transfer through aggregate interlock action. Current design methods for shear do not take the aggregate type into consideration. This paper describes a series of non-linear finite element analyses the authors carried out to assess the influence of crack roughness on the shear strength of beams. The models incorporated both smeared and discrete cracking elements. The numerical models were validated with data from 22 beams tested at Imperial College London. In general, the ultimate load, crack patterns and relative crack displacements were satisfactorily reproduced. The reduction in strength due to aggregate fracture was found to be greatest in slender beams without stirrups and insignificant in short span beams where the cracks tended to open rather than slide.

### Streszczenie

Badania doświadczalne wskazują, że w betonie wysokiej wytrzymałości siły przyczepności pomiędzy kruszywem i zaczynem cementowym mogą być na tyle duże aby zarysowanie powstawało w kruszywie. Rysy przechodzące przez kruszywo są gładkie i znacząco redukują zdolność do przenoszenia sił tnących poprzez ząbkowanie się kruszywa. W artykule przedstawiono nieliniowe analizy numeryczne, przeprowadzone przez autorów w celu oceny wpływu charakteru zarysowania na nośność na ścinanie belek. Analizy wykonano zarówno dla modelu z rozmytym jak i dyskretnym obrazem zarysowania. Modele numeryczne zostały porównane z wynikami badań 22 belek. Największe obniżenie nośności na ścinanie spowodowane zniszczeniem kruszywa obserwowano w belkach smukłych, nie zbrojonych strzemionami.

Keywords: Aggregate interlock; High-strength concrete; Non-linear finite element analysis; Shear design.

## 1. INTRODUCTION

The coarse aggregate can fracture at cracks in high-strength concrete (HSC) due to the strong bond between the aggregate and the cement paste. The authors tests showed that limestone aggregate can fracture in beams with concrete cube strengths as low as 60MPa, resulting in smooth crack surfaces as shown in Fig. 1a. The consequences of smoother cracks and the subsequent reduction in aggregate interlock action are not well understood for HSC. Design codes do not realistically account for the effect of variations in aggregate type on shear strength. Instead simplified

approaches are used to take into account aggregate fracture such as reducing the concrete strength or aggregate size used in shear calculations. In reality, the contribution of aggregate interlock to shear strength depends on the crack pattern and the crack relative displacements which in turn depend on the ratios of shear span to effective depth ( $a/d$ ) and shear reinforcement ( $\rho_w$ ).

Modifications have been previously proposed [1] to MC90 to account for the reduction in shear strength due to the fracture of aggregate particles but insufficient information is given to implement the method in

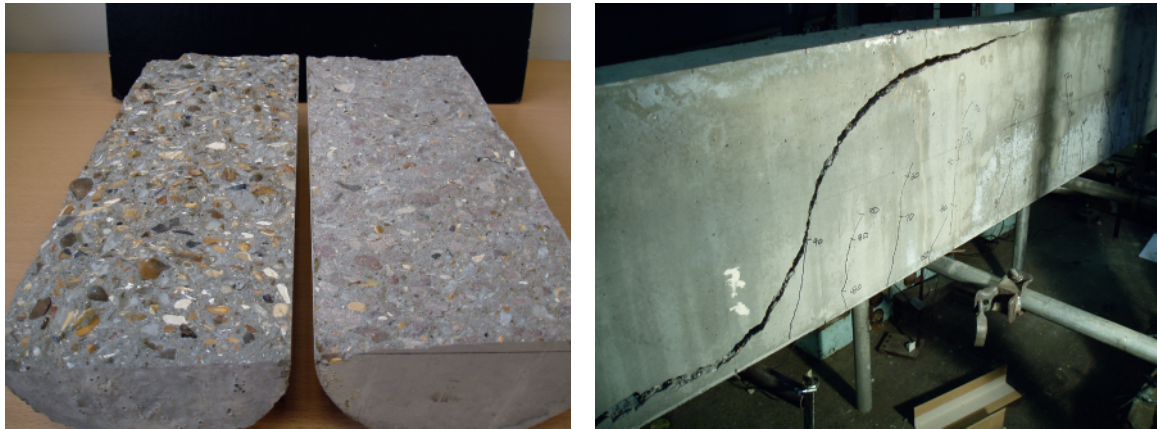


**Figure 1.** (a) Crack surfaces in gravel (left) and limestone (right) aggregate concretes; (b) Shear failure of limestone aggregate concrete beam (smooth cracks)

practice. Sheerwood et al. [2] proposed that the effects of aggregate fracture should be modelled indirectly by reducing the aggregate size in analyses with the MCFT of Vecchio & Collins [3]. The “effective” aggregate size considered in the model is estimated through an empirical formula which only depends on the concrete strength and not the aggregate type.

The shear response of reinforced concrete beams is still uncertain due to the large number of variables involved. Various analytical and numerical procedures have been used in recent years to obtain a better understanding of these mechanisms. Many different constitutive material models have been developed for use in non-linear finite element analysis (NLFEA). These models are being continually revised and updated in response to the development of high performance concretes. Numerical difficulties can be expected in the NLFE modelling of shear critical concrete structures due to their brittle behaviour and the large number of parameters involved. Smearred cracking models are widely accepted for the NLFEA of reinforced concrete structures and can provide good predictions of the crack pattern and general behaviour of shear critical reinforced concrete beams. However, discrete crack models are required to accurately model aggregate interlock.

The NLFE models presented in this paper were used to investigate the influence of aggregate fracture on the shear strength of reinforced high-strength concrete beams. The NLFEA was carried out using the commercially available software package DIANA v.9. The paper reviews the performance of three commonly used smearred crack approaches (i.e. fully rotating, multi-fixed and totally fixed crack). Combined models using smearred and discrete crack

elements are also used to examine the relative displacements at cracks in beams tested by the authors.

## 2. EXPERIMENTAL PROGRAMME

Most existing experimental evidence on the influence of aggregate interlock is from tests on slender beams without shear reinforcement, e.g. Regan [5], Taylor [6]. The influence of aggregate fracture on the shear strength of slender beams with stirrups and short span beams is less certain since the type of aggregate and whether it fractured is seldom reported. Two series of tests were performed at Imperial College London to assess the influence of aggregate fracture on shear strength; namely Series I with slender beams ( $a/d=3.5$ ) without shear reinforcement and Series II with short span beams ( $a/d=1.5$ ) with and without stirrups. The geometrical and material properties of

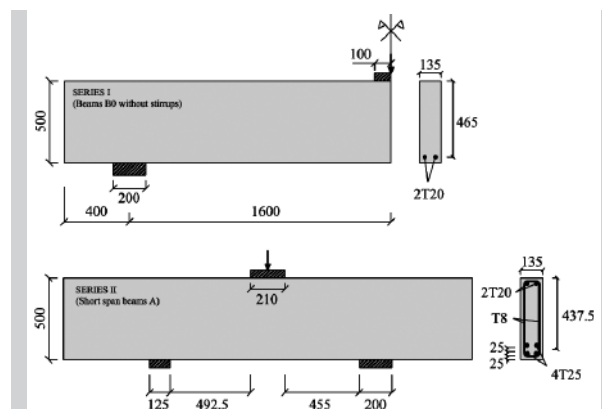


**Figure 2.** Geometry of beams tested by the authors (Sagasetta [7]); (a) Slender beams without stirrups (Series I); (b) Short span beams (Series II)

the beams are summarised in Table 1. Sagaseta [7] gives full details of the tests elsewhere. Beams denoted “0” had no shear reinforcement. The beams were all 500 mm deep and 135 mm wide as shown in Fig. 2.

The beams were constructed in pairs with one set cast from normal gravel aggregate concrete (denoted as “G”) and the other set from concrete with limestone coarse aggregate (denoted as “L”). The aggregate fractured completely in the beams with limestone aggregate unlike the beams with gravel aggregate where the crack only went through a small proportion (~30%) of the aggregate, as shown in Fig. 1a.

The beams were simply supported and loaded at mid-span. The loading plates were 200 mm long and 135 mm wide in all the tests, except for Series II where the length of one of the support bearing plates was reduced to 125 mm to encourage failure in that shear span. The distance  $a$  between the centrelines of the load and adjacent support was 1600 mm in Series I and 660 mm in Series II. All the beams failed in shear though the flexural reinforcement yielded in beams AG3 and AG4. The flexural reinforcement ratios were 1% and 3.32% in Series I and II respectively.

**Table 1.**  
Summary of experimental results of Series I and II

Beam	$f_c'$ [MPa]	$\rho_w \cdot f_{yw}$ [MPa]	$V_{test}$ [kN]
<i>Series I (a/d=3.4)</i>			
BG0-1	80.2	-	61.3
BG0-2	80.2	-	63.1
BL0-1	68.4	-	46.9
BL0-2	68.4	-	54.1
<i>Series II (a/d=1.5)</i>			
AG0	80.2	-	325.8
AG2	80.2	1.24	563.0
AG3	80.2	1.86	654.6
AG4	80.2	2.48	707.1
AL0	68.4	-	365.5
AL2	68.4	1.24	531.9
AL3	68.4	1.86	480.7
AL4	68.4	2.48	602.2

Notes: \*  $\rho_w = 100A_{sw}/(ab)$

where  $A_{sw}$  = area of stirrups;  $b$  = width;  $s$  = stirrup spacing

The mode of failure and crack patterns were significantly different in Series I and II as expected. The crack opening ( $w$ ) and sliding ( $s$ ) displacements were measured in test Series II to determine the contributions of aggregate interlock to the ultimate shear strength. The authors also carried out push-off tests in specimens with the same aggregates as in beam

tests to assess the relationship between crack opening, sliding and shear stress along cracks crossed by a similar number of stirrups as in the beams.

### 3. SMEARED AND DISCRETE CRACK MODELLING IN NLFEA

Smeared and discrete crack formulations are widely used for modelling cracking in concrete. In the smeared crack approach, cracking is smeared within the element unlike the discrete approach where a gap is introduced into the mesh after cracking. The discrete crack approach is more realistic than the smeared crack formulation but it is far more complicated to implement in a finite element model since it requires the nodal connectivity to be changed on crack formation. Furthermore, the crack must follow the element edges. The smeared method idealises the cracked element as a continuum which can lead to “stress locking” effects near the crack. These local effects are usually unimportant and the general behaviour of the structure can be well predicted with smeared models. A combined smeared/discrete crack approach was considered most suitable for the present work where the main objective was to assess the relative opening and sliding displacements and shear transfer at cracks.

A preliminary analysis was performed using only elements incorporating smeared cracking in order to estimate the location of the principle shear cracks and to validate the smeared models with experimental data. Three of the smeared cracking models included in DIANA were examined: namely the total strain rotating crack, total strain fixed crack and multi-fixed models. The first two models are based on a total strain concept similar to the MCFT whilst the third model combines strain decomposition ( $\epsilon_{elastic} + \epsilon_{crack}$ ) in tension with an elasto-plastic model in compression, as described in [8]. The multi-fixed model utilises a multi-directional fixed crack technique which incorporates the extreme cases of fully rotating and totally fixed cracks dependent on the choice of threshold angle at which further cracking is permitted.

Once the crack location and the smeared models were validated they were implemented in a combined smeared/discrete FE model where interface elements were introduced to account for aggregate interlock. All the models shown in this paper are two-dimensional consisting of plane-stress elements with quadratic interpolation, i.e. 8 and 6 node elements for quadrilateral and triangular elements respectively. A Gauss integration scheme of  $2 \times 2$  for the quadri-

lateral elements and 3-point for the triangular elements was applied. The loading plates were included in the FE mesh to avoid local concentration of stresses in the concrete. A regular Newton-Rapson incremental-iterative procedure for the non-linear analysis was used. An energy norm criteria (1%) was applied for the iteration process. The load was applied in displacement control with constant steps of 0.1 mm.

#### 4. VALIDATION OF SMEARED CRACKING MODELS IN THE NLFEA

##### 4.1. Slender beams without stirrups (Series I)

The experimental results from the slender beams without shear reinforcement (Series I) correlated well with those of Regan [5] who tested beams with similar types of aggregate. Identical failure modes were observed for the limestone and normal gravel beams. Failure occurred suddenly after the formation of the critical diagonal crack which extended horizontally into the compression zone and along the flexural reinforcement towards the support as shown in Fig. 1b. The failure crack surface was smoother for BL0 than for BG0. The influence of aggregate fracture on the shear strength of slender beams without stirrups was examined using equation (1) below from EC2 [4] with material factors of safety ( $\gamma_c$ ) equal to 1:

$$V_{Rd,c}(EC2) = 0.18/\gamma_c \cdot (100 \cdot \rho_l \cdot f_c')^{1/3} \cdot (1 + \sqrt{200/d}) \cdot b \cdot d \quad (1)$$

where  $\rho_l$  = longitudinal reinforcement ratio;  $f_c'$  = cylinder compressive strength;  $d$  = effective depth; and  $b$  = width. The  $V_{Rd,c}/V_{test}$  ratio using (1) was 16% larger for the limestone beams than for the normal gravel beams due to aggregate fracture.

Beams in Series I were modelled using the three smeared cracking approaches described in section 3 (i.e. total strain fixed, total strain rotating, multi-fixed). A shear retention factor  $\beta$  of 0.1 was used in both the totally fixed and the multi-fixed models. The threshold angle ( $\alpha$ ) was selected as 30° in the multi-fixed model. The remaining material properties considered in the models are summarized in Table 2. The concrete elastic modulus ( $E_c$ ), tensile strength ( $f_{ct}$ ), compressive strength ( $f_c'$ ) and the steel yield strength ( $f_y$ ) were obtained experimentally whilst the remaining parameters were estimated. The strain-stress models used were the Hordijk [8, 9] softening curve for tension and a parabolic curve proposed by

Feenstra [10] for compression, which are defined by respective tension and compression fracture energy given in Table 2.

**Table 2.**  
Material properties in NLFEA

Concrete	BG0	BL0
$E_c$ [GPa]	42.6	35
$\nu$	0.2*	0.2*
$f_{ct}$ [MPa]	5.7	4.9
$G_f$ [N/mm]	0.113	0.101
$f_c$ [MPa]	80.2	68.4
Steel	Type 1	Type 2
$E_s$ [GPa]	200	200
$\nu$	0.3	0.3
$f_y$ [MPa]	550	580

Notes: \* In the Total Strain models  $\nu = 0$   
+  $G_c = 100G_f$  was assumed  
where  $G_f$  (MC90) =  $G_{f0} \cdot (f_{cm}/f_{cm0})^{0.7}$   
Steel Type 1: transverse reinf. and plates  
Steel Type 2: longitudinal reinf.

The total strain fixed crack model incorrectly predicted flexural failure and consequently overestimated the failure load (Table 3). The use of totally fixed crack models within a total strain formulation can give inconsistent results in cases where cracks cross previous cracks with different inclinations. On the other hand, the total strain rotating and multi-fixed models predicted the ultimate load and mode of failure satisfactorily as shown in Table 3. However, numerical difficulties were faced near the measured failure loads as discussed below.

**Table 3.**  
NLFEA predictions of ultimate strength of slender beams without stirrups using different smeared cracking models

Beam	$V_{test}/V_{calc}$		
	NLFEA Tot. Fix	NLFEA Tot. Rot	NLFEA Multi-fix
BG0	0.57	1.02	1.01
BL0	0.45	1.06	0.87
Mean	0.51	1.04	0.94
COV.	0.16	0.02	0.11

Note:  $V_{test}$  is the average between B01 and B02

The iterative procedure used in the multi-fixed model diverged close to the measured value (Fig. 3). Divergence of an iterative process in NLFEA is not always associated with failure, but in this case it appears to be related to the sudden formation of the diagonal crack.

The total strain rotating model provided sensible predictions for the failure load and crack pattern but the predicted post-failure response was unrealistic as shown in Fig. 3. Failure in the total strain rotating model was assumed at the load step in which the diagonal crack was predicted to form. This critical step also corresponded to a considerable increase in vertical deflection; refer to circle marks in Fig. 3. A considerable increase in load was predicted after this point, which is inconsistent with the experimental evidence. This spurious load branch, which is partially shown in Fig. 3, is denoted as “post-failure behaviour”.

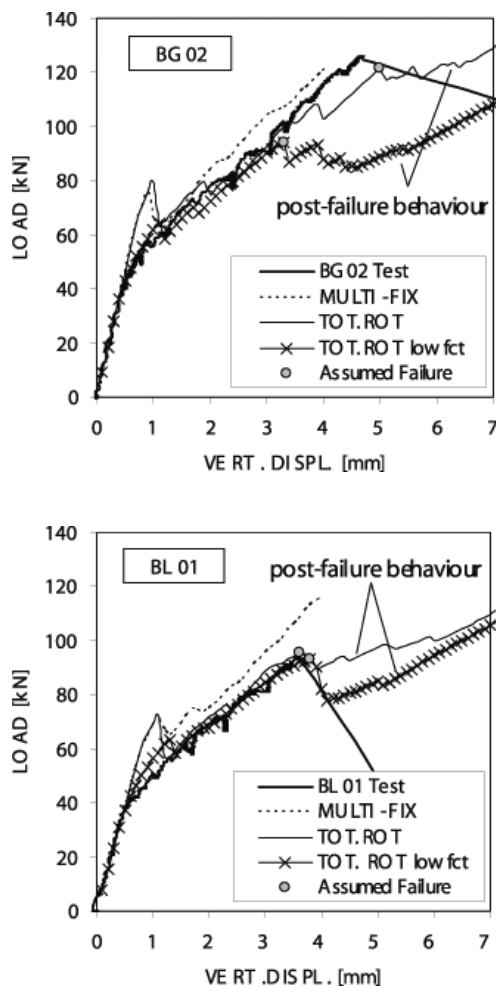


Figure 3. Load-deflection prediction using smeared models for slender beams without shear reinforcement

The increment in load obtained in the post-failure branch was accompanied by the development of a

horizontal smeared crack along the longitudinal reinforcement as shown in Fig. 4. The spurious load mechanism appears to be related to the complete debonding of the concrete from the longitudinal reinforcement at failure which is not accurately modelled in the NLFEA model.

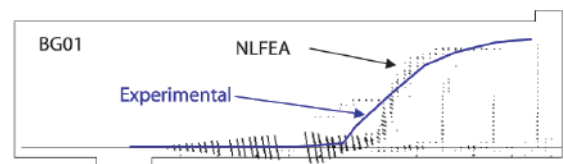


Figure 4. NLFEA (total strain rotating) crack pattern predictions; “post-failure behaviour”

The concrete tensile strength ( $f_{ct}$ ) has a significant effect on the predicted response of slender shear critical beams without shear reinforcement as reported by Vecchio and Shim [11]. In the previous analyses,  $f_{ct}$  was obtained from cylinder splitting tests. This provided good estimates of ultimate loads but the first flexural cracks formed later in the analyses than in the tests. The prediction of the initial crack development was improved if the tensile strength was reduced to  $f_{ct}=0.33(f_c')^{1/2}$  as recommended by Bresler and Scordelis [12] but the ultimate load was underestimated in some cases such as beam BG02 (see “Tot. Rot low  $f_{ct}$ ” in Fig. 3).

The NLFEA presented here did not model the effect of aggregate fracture. Hence, the predicted strengths were expected to be less conservative for BL0 than for BG0. However, this was only true for the multi-fixed model. This was probably due to differences in the concrete properties (e.g.  $f_c$  and  $f_{ct}$ ) used for each set of beams in the numerical models which had a significant effect on the numerical predictions.

#### 4.2. Short span beams (Series II)

The performance of the smeared cracking models studied in the previous section was investigated for the eight short span beams tested in Series II. The material properties used in the analyses are given in Table 2. Table 4 compares the results from the NLFEA with the predictions of the design recommendations for short span beams in EC2 (clause 6.2) and a strut-and-tie model (STM) developed by the authors [13].

The mode of failure in shear is significantly different

for short span beams than slender beams. The main diagonal crack forms independently of the flexural cracks in short span beams unlike slender beams without stirrups where the formation of the principle shear crack precipitates sudden failure. The critical diagonal crack, which ran in an almost straight line between the inner edges of the loading plates in the authors' short span beams, formed at around 30% of the ultimate load and remained stable until failure. Failure of the short span beams was due to either splitting or crushing of the concrete above the main crack near the loading plate.

**Table 4.**  
Summary of ultimate strength predictions of short span beams

Beam	$V_{test}$ [kN]	$V_{test}/V_{calc}$				
		EC2 [4]	STM-EC2 [13]	NLFEA Tot. Fix	NLFEA Tot. Rot	NLFEA Multi-fix
AG0	325.8	0.53	1.27	0.97	0.97	0.95
AG2	563.0	0.35	0.82	0.79	0.65	0.90
AG3	654.6	0.45	0.73	0.71	0.59 <sup>+</sup>	0.82
AG4	707.1	0.56	0.71	0.70	0.67	0.53 <sup>+</sup>
AL0	365.5	0.45	1.04	0.80	0.97	0.80
AL2	531.9	0.37	0.79	0.75	0.65	0.98
AL3	480.7	0.61	0.92	0.89	0.76	0.97
AL4	602.2	0.65	0.77	0.71	0.74	0.83
	Mean	0.50	0.88	0.79	0.75	0.84
	COV.	0.22	0.25	0.12	0.20	0.20

Note: + Analysis stopped prematurely

The accuracy of the predicted failure load of the short span beams was improved if the concrete tensile strength  $f_{ct}$  was reduced in the NLFEA unlike the slender beams where the converse was true. Reducing  $f_{ct}$  to 2.95 and 2.70 MPa for the AG and AL series of beams respectively in accordance with [12] was found to significantly improve the predictions of crack development and ultimate load, especially for the beams without stirrups (A0). The load-deflection response became excessively stiff when the measured values of  $f_{ct}$  given in Table 2 were used in the analysis. This over-stiff behaviour arose since the principle shear crack in the NLFEA formed below the actual position of the crack in the tests and had a break point in the middle where the slope changed suddenly.

The multi-fixed model gave the best predictions of the three smeared models investigated. The total strain fixed and rotating models provided very similar results to each other due to the limited crack rotation within the shear span of the short span beams. The

total strain models exhibited a spurious post-failure response due to the formation of new cracks on top of the main diagonal crack near the loading plate. Good predictions of the load-deflection curves were obtained up to failure for most of the beams. However, in some specimens the ultimate load was underestimated due to local failure of the elements near the loading plate (beams AG4 and AG3, see Table 4). No attempt was made to improve the predictions of the ultimate load since the primary aim of the analyses was to investigate which of the smeared crack models was most suitable for implementation into the combined smeared/discrete crack models shown in section 5.

## 5. COMBINED SMEARED/DISCRETE CRACKING NLFE MODELS

### 5.1. Description of the finite element model

Once the smeared crack models were validated, they were implemented into a more refined FE mesh to determine the displacements along the main diagonal crack. Linear interface elements were placed in the mesh (Fig. 5) in order to model aggregate interlock along the crack surfaces. A multi-fixed smeared crack model was adopted for the concrete elements. Feenstra et al. [14] have reported that numerical oscillations can occur in interface elements with small thicknesses and that the problem can be solved by applying Newton-Cotes quadrature elements. Hence, 6-node interface elements were used with a 3-point Newton-Cotes integration scheme (Fig. 5). The reinforcement was modelled as in previous models using embedded elements assuming perfect bond between the steel and the concrete. The special considerations described below had to be made regarding the normal and transverse stiffness of the reinforcement elements crossing the interface plane.

In order to keep the model numerically stable, a simple discrete crack constitutive model was used for the interface elements in which cracking was initiated when the concrete tensile strength was reached. In addition, the tensile and shear stresses were assumed to be uncoupled in the open crack. A linear softening curve was used for cracked concrete in tension in conjunction with a constant shear retention factor within the interface elements once cracking had initiated. The overall shear stiffness after cracking assigned to the interface elements, which is attributed to aggregate interlock and dowel action, was estimated using the simple formula suggested by Hamadi and Regan [15] ( $D_T=k/w$ ) with  $k=5.4\text{MPa}$



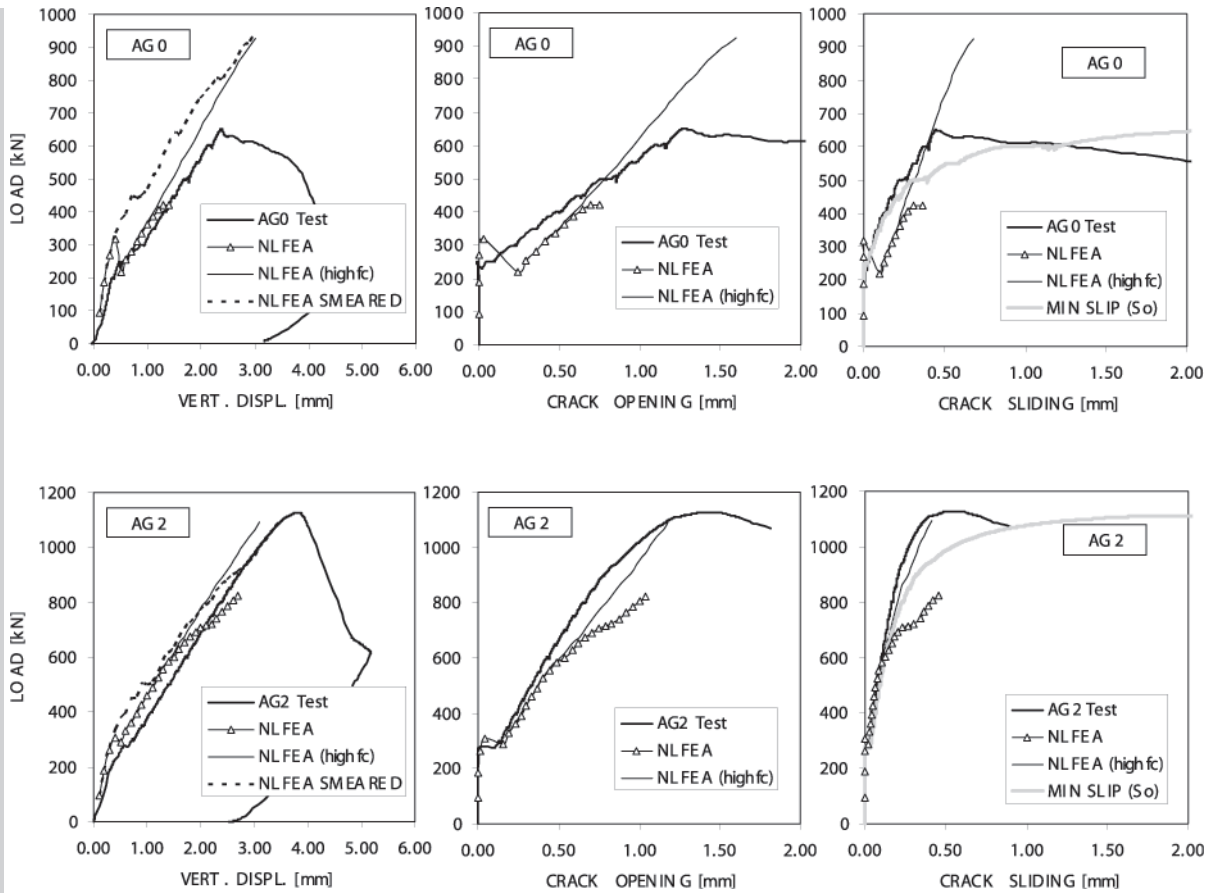


Figure 6. Load-deflection curves and crack opening/sliding of beams AG0 and AG2

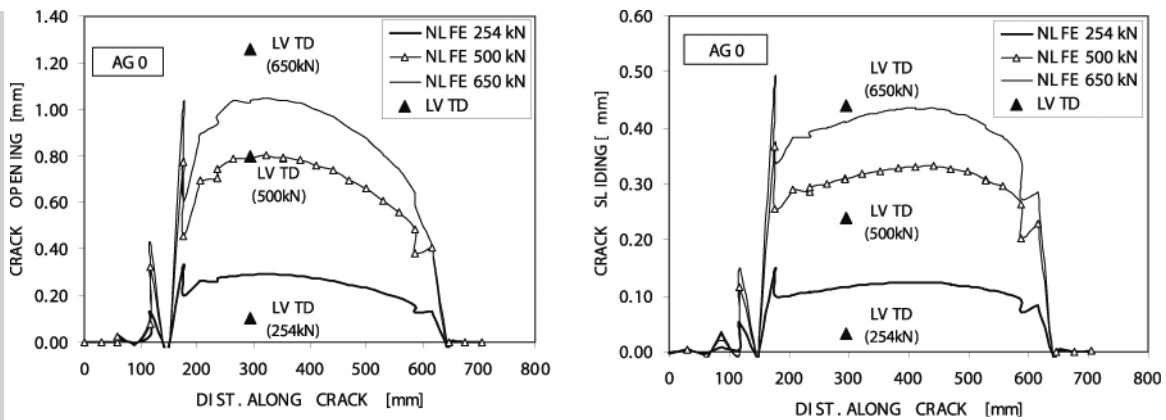


Figure 7. Crack opening and sliding along discrete crack in beam AG0

The numerical values shown in Fig. 6 correspond to the maximum value at the interface element nearest to the cross of LVDT's. This element was located in between two stirrups at a distance of 295 mm from the bottom of the discrete crack. As shown in Fig. 7,

the predicted crack slip was constant along the discrete crack plane in beams with and without stirrups. The crack opening predicted in the NLFEA was fairly uniform in beams without stirrups. Interface elements crossed by longitudinal reinforcement

remained inactive (i.e.  $w$  and  $s$  were negligible). In beams with stirrups, the predicted crack opening was uniform at early load stages while for loads near failure  $w$  was considerably lower at interface elements crossed by shear links. In reality, the crack widths observed in the experiments followed a more uniform profile due to bond slip at the stirrups which was not accounted for in the NLFEA.

In all the short span beams, the measured crack opening ( $w$ ) was predominant over sliding ( $s$ ) up to failure with a  $\delta_w/\delta_s$  ratio around 3, as shown in Fig. 8. This ratio was consistent with the predictions of the NLFEA as shown in Fig. 8 and suggests that little shear stress was transmitted through the principle shear crack in the authors' short span beams (i.e. Series II). It is also noteworthy that the crack opening and sliding displacements at failure were similar in all beams. Sliding only became significant after the ultimate load was reached and the  $\delta_w/\delta_s$  ratio reduced to close to 1.

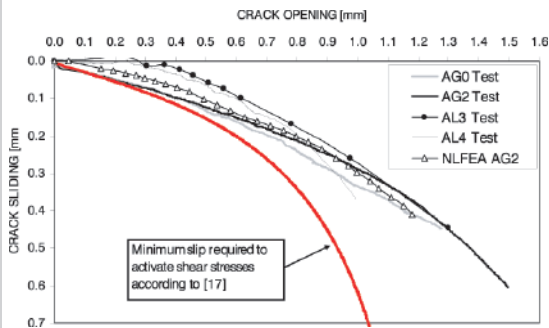


Figure 8. Crack opening-sliding relationship for short span beams tested

5.3. Numerical predictions of slender beams with stirrups

Combined discrete/smeared crack finite element models, similar to the one shown in the previous section for short span beams were developed for continuous beams with stirrups (Sagasetta [7]). Fig. 9a shows the FE mesh used in this case, which contains several discrete shear cracks. The location and geometry of these cracks was obtained after testing the specimens, although preliminary analysis using smeared cracking only, provided a good estimation of the crack pattern (Fig. 9b).

The predictions of the crack opening and sliding displacements were reasonable (Sagasetta and Vollum [16]). The results were consistent with experimental

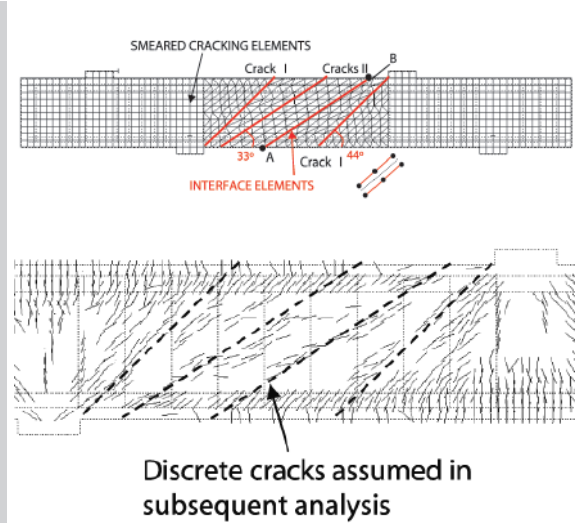


Figure 9. (a) FE mesh of continuous beam with stirrups (critical crack between points A-B); and (b) Crack pattern predicted a priori in central span using smeared crack elements only

finding which showed that crack opening was less dominant in the slender beams than the short span beams. The slip was predicted to be fairly uniform along the active discrete crack as in the NLFEA of the short span beams. The crack opening was slightly underestimated in some cases at loads near failure and the predicted crack width  $w$  reduced locally at interface elements crossed by stirrups as shown in Fig. 10. Good agreement was obtained between crack widths obtained from the crosses of LVDTs, digital photogrammetry and visually. The readings were self consistent and showed a fairly uniform distribution of  $w$  even for loads near failure (Fig. 10).

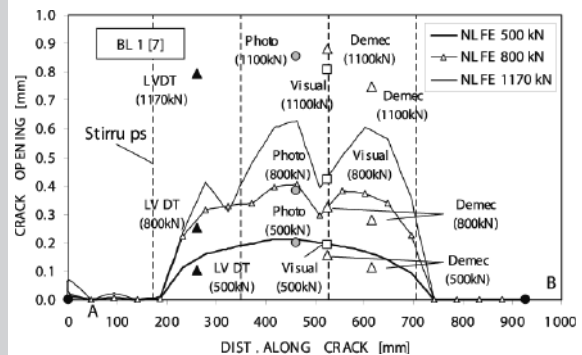


Figure 10. Crack opening along discrete crack (A-B) in continuous beam with stirrups

#### 5.4. Final remarks on constitutive models for discrete cracking (interface elements)

In the previous combined smeared/discrete analysis, aggregate interlock was modelled with a highly simplistic constitutive model. In reality aggregate interlock is much more complex since it involves an interaction between normal and shear stresses. In addition, the stiffness of the interface is not constant after the crack opens, as assumed in the previous models, since it decreases as the crack opens. Hence, the increase in  $w$  and  $s$  near failure could not be captured using a constant aggregate interlock stiffness model, as shown in Fig. 6.

Many crack dilatancy models are available for use in NLFEA which can account for these aspects in a more realistic manner. Crack dilatancy models have been reported to be numerically unstable (Feenstra et al. [14]) so empirical formulations such as the linear aggregate interlock relationship (Walraven and Reinhardt [17]) are commonly applied due to their simplicity. According to Walraven and Reinhardt's relationship, shear is only transferred through cracks once the slip exceeds a critical value ( $S_o$ ) which depends on the crack width.  $S_o$  was calculated at each load step in terms of the crack width measured in the short span beams. The measured sliding displacements were less than  $S_o$  (see Fig. 6 and 8), which suggests that the shear stresses were relatively low along the crack and that the use of complex crack dilatancy models is not justified for this particular case. The simple approach of using a constant shear retention factor after cracking seems more questionable for slender beams since the  $\delta_w/\delta_s$  ratio was lower than in the short span beams. However, it has been shown [7] that sensible predictions can be obtained if the shear stiffness of the discrete crack is calibrated beforehand using appropriate analytical formulae or data from push-off tests.

## 6. CONCLUSIONS

This paper presents a simple procedure for assessing relative crack displacements using combined smeared and discrete crack finite element modelling. The numerical models, which were assembled in DIANA, converged in relatively few iterations and provided useful information at both local (crack) and global (beam) levels. The crack opening/sliding and stiffness of the short span and slender beams tested were successfully reproduced using a simple discrete crack constitutive model for the interface elements and a multi-fixed smeared cracking model for the concrete. These models were used to investigate the influence of aggregate interlock action on the shear response of reinforced high-strength concrete beams which is still not fully understood. The ratio  $V_{Rd,c}/V_{test}$  was calculated with EC2 for the slender beams without stirrups tested in this programme. The ratio was found to be 16% larger for the beams with limestone aggregate than for comparable beams with gravel aggregate due to aggregate fracture. The authors did not observe any reduction in shear strength due to aggregate fracture in their beams with shear reinforcement but more tests are required to establish this conclusively. Aspects such as aggregate fracture, which is shown to be more critical in slender beams without shear reinforcement, are not treated in a rational manner by design codes and future work is required.

The performance of smeared cracking models should be verified experimentally before implementing the models into combined smeared/discrete NLFEA. Although combining smeared and discrete cracking elements can provide accurate predictions, the models assumed for smeared cracking, crack interface, dowel action and bond-slip relationships must incorporate both realistic behaviour and numerical simplicity. This is especially important in modelling of shear critical high-strength beams since the type of failure can be extremely sudden.

## ACKNOWLEDGEMENTS

The authors would like to thank the staff of the Concrete Structures Laboratory at Imperial College and acknowledge the financial support of Fundación Caja Madrid.

## REFERENCES

- [1] *CEB*; High performance concrete, recommended extensions to the Model Code 90, research needs. CEB Bulletin d'Information, Report 228, July 1995
- [2] *Sherwood E. G., Bentz E. C., Collins M. P.*; Effect of aggregate size on beam-shear strength of thick slabs. *ACI Structural*, Vol.104, No.2, March-April 2007, p.180-190
- [3] *Vecchio F. J., Collins M. P.*; The modified compression-field theory for reinforced concrete elements subjected to shear. *ACI Structural*, No.83-22, October 1986, p.219-231
- [4] *British Standards Institution*; European Standard EN-1992-1-1:2004, Eurocode 2: Design of Concrete Structures. Part 1, General Rules and Rules for Buildings. BSI, 2004, London
- [5] *Regan P. E., Kennedy-Reid I. L., Pullen A. D., Smith D. A.*; The influence of aggregate type on the shear resistance of reinforced concrete. *The Structural Engineer*, December 2005, p.27-32
- [6] *Taylor H. P. J.*; Investigation of the forces carried across cracks in reinforced concrete beams in shear by interlock of aggregate. CCA, London, November 1970
- [7] *Sagaseta J.*; The influence of aggregate fracture on the shear strength of reinforced concrete beams. PhD Thesis, Department of Civil & Environmental Engineering, Imperial College London, 2008
- [8] *TNO DIANA BV*; User's Manual Release Notes. Frits C. de Witte and Gerd-Jan Schreppers (Eds.), Delft 2005
- [9] *Cornelissen H. A. W., Hordijk D. A., Reinhardt H. W.*; Experimental determination of crack softening characteristics of normalweight and lightweight concrete. *Heron*, Vol.31, 1986
- [10] *Feenstra P. H.*; Computational aspects of biaxial stress in plain and reinforced concrete. PhD Thesis, Delft University of Technology, 1993
- [11] *Vecchio F. J., Shim W.*; Experimental and analytical re-examination of classic concrete beam tests. *Journal of Structural Engineering*, Vol.130, No.3, March 2004, p.460-469
- [12] *Bresler B., Scordelis A. C.*; Shear strength of reinforced concrete beams. *Journal of American Concrete Institute*, Vol.60, No.1, 1963, p.51-72
- [13] *Sagaseta J., Vollum R.*; Shear design of short span beams. *Magazine of Concrete Research* (paper accepted for publication in June 2009)
- [14] *Feenstra P. H., De Borst R., Rots J. G.*; Numerical study on crack dilatancy I: Models and stability analysis. *Journal of Engineering Mechanics*, Vol.117, No.4, April 1991, p.733-753
- [15] *Hamadi Y. D., Regan P. E.*; Behaviour of normal and lightweight aggregate beams with shear cracks. *The Structural Engineer*, 58B(4), 1980, p.71-79
- [16] *Sagaseta J., Vollum R.*; Relative crack displacements in high strength concrete beams failing in shear. *Proceeding of the 11<sup>th</sup> International fib Symposium*, London, 2009
- [17] *Walraven J. C., Reinhardt H. W.*; Theory and experiments on the mechanical behaviour of cracks in plain and reinforced concrete subjected to shear loading. *Heron*, Vol.26, No.1(a), 1981, p.5-68

